A 98.7% Efficient Composite Converter Architecture With Application-Tailored Efficiency Characteristic

Hua Chen, *Student Member, IEEE*, Kamal Sabi, Hyeokjin Kim, *Student Member, IEEE*, Tadakazu Harada, Robert Erickson, *Fellow, IEEE*, and Dragan Maksimovic, *Fellow, IEEE*

***Abstract*—A dc–dc boost composite converter architecture is introduced that can lead to optimized efficiency over a range of operating points dictated by the application requirements. The composite converter system employs dissimilar modules to minimize the ac power losses in the indirect power conversion paths. It is composed of three converter modules: buck converter, boost converter, and a dual active bridge converter that operates as a dc transformer (DCX). Each module processes partial power, with reduced voltage rating. With the same semiconductor area and same magnetics volume, substantial efficiency improvements and reductions in capacitor size are achieved relative to a conventional boost architecture. It is possible to design each module to optimize efficiency over a wide operating range, including pass-through modes that exhibit very low loss. A 10-kW boost composite converter is experimentally demonstrated having 98.7% efficiency at a critical partial power point, with similar very high efficiencies achieved over a wide operating range.**

***Index Terms*—Boost converter, composite converter, dc–dc converter, high efficiency, modular systems.**

I. Introduction

TODAY many power electronic applications require efficiency optimization at certain critical operating points, instead of optimizing efficiency at full power. For example, power converters for solar power systems are characterized by a weighted efficiency that accounts for efficiency not only at rated power but also at lower powers corresponding to less than full irradiance [1], [2]. Power converters for electric vehicle applications must operate over driving profiles having a wide variety of speeds and accelerations, corresponding to a variety of converter output voltages and powers; improvement of efficiency at all of these operating points is needed to improve the miles-per-gallon-equivalent in standard driving cycle tests [3]. Power converters for grid interface of variable-speed wind turbines must also operate efficiently with a wide range of voltages and output powers, corresponding to a range of wind speeds. In the literature, various methods have been proposed to improve dc–dc converter efficiency [4]–[9]. However, very few of these emphasize optimization of efficiency at specific critical operating points or ranges.

In voltage step-up applications, it is well known that the performance of the traditional boost dc–dc converter is poor when operating with high boost conversion ratios. At high duty cycles, the boost converter exhibits poor efficiency, high capacitor rms current, and large semiconductor voltage and current stress.

In this study, a new *composite* boost dc–dc architecture is introduced, in which dissimilar converter modules are combined into a system having performance superior to that of the individual modules. This approach enables optimization of efficiency at specified critical operating points, as well as substantial improvement of efficiency over a wide operating range. Voltage stresses are shared between series-connected modules, enabling use of lower-voltage semiconductors having higher switching speed and lower forward voltage drop. The composite converter system architecture transmits the required indirect power with efficiency that is optimized over a wide range of operating points. Each of these modules can operate either with normal PWM or in pass-through or shut-down mode. The new composite architecture allows new degrees of freedom in power component optimization and in control strategy to achieve substantially higher efficiencies at key operating points and over a wide operating range. Additionally, the proposed composite architecture also has the potential to reduce total capacitor volume.

The organization of this paper is as follows. In Section II, the step-up composite converter architecture is proposed, and its operating details are discussed. In Section III, an example 10-kW composite converter is designed and its optimization is discussed. Performances of the composite converter and conventional boost converter are compared in Section IV. Performance of an experimental prototype composite converter is documented in Section V. Conclusions are summarized in Section VI.

II. New Boost Composite Converter Architecture

It is well known that the efficiency of the conventional boost converter is high when conversion ratio $M = V_{\rm out}/V_{\rm in}$ is close to one [10]. As duty cycle increases, conversion ratio increases and efficiency drops. Typically, ac loss mechanisms such as switching loss, inductor core loss, and winding proximity loss, are greater than the dc conduction losses and hence the ac loss mechanisms dominate the total loss.

Fig. 1 illustrates a conventional boost converter and an averaged switch model [10] of the dc and low-frequency waveform

Manuscript received October 18, 2014; revised December 10, 2014; accepted January 15, 2015. Date of publication February 3, 2015; date of current version September 21, 2015. Recommended for publication by Associate Editor G. Moschopoulos.

H. Chen, H. Kim, R. Erickson, and D. Maksimovic are with the Department of Electrical, Computer and Energy Engineering, University of Colorado, Boulder, CO 80309 USA (e-mail: hua.chen@colorado.edu; hyeokjin.kim@colorado.edu; robert.erickson@colorado.edu; maksimov@colorado.edu).

K. Sabi is with the Techneaux, Lafayette, LA 70506 USA (e-mail: kamal.sabi@colorado.edu).

T. Harada is with the Toyota Motor Corporation, Toyota City 471-8571, Japan (e-mail: tadakazu.harada@colorado.edu).

Color versions of one or more of the figures in this paper are available online at http://ieeexplore.ieee.org.

Digital Object Identifier 10.1109/TPEL.2015.2398429

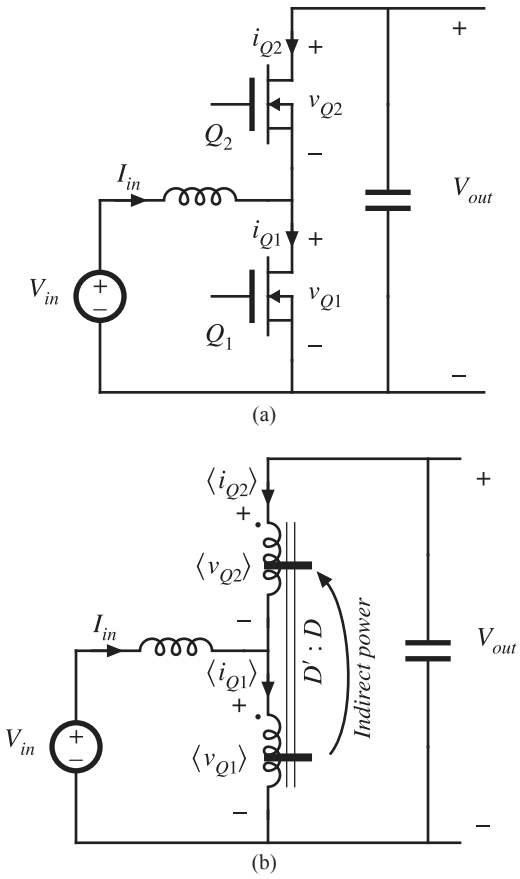

Fig. 1. Conventional boost converter. (a) Schematic. (b) Averaged switch model.

components for an ideal lossless converter. In this model, the effective dc transformer represents the *indirect power flow* within the converter. This indirect power is the power that is converted from dc to ac (switching frequency) power by transistor Q_1. This indirect power then rectified by synchronous rectifier Q_2 and hence converted back to dc. The switching-frequency components of the waveforms are excluded from the averaged model of Fig. 1(b); rather, this model simply illustrates the effective consumption of dc power by Q_1 and effective generation of dc power by Q_2. The angle brackets denote averaging over one switching period to extract the dc or low-frequency component. By solution of the averaged switch model, we find that this indirect power is equal to

$$P_{\text{indirect}} = \langle\, v_{Q1}\,\rangle\langle\, i_{Q1}\,\rangle = DV_{\text{in}}I_{\text{in}}. \tag{1}$$

Indirect power is the mechanism by which boost converters achieve voltage gain, and also by which buck converters achieve current gain. Thus, indirect power flow is a key underlying feature of any high-efficiency power converter [11].

The dc power produced by the synchronous rectifier is

$$-\langle\, v_{Q2}\,\rangle\langle\, i_{Q2}\,\rangle = \eta_{ac}P_{\text{indirect}} \tag{2}$$

where η_{ac} is the efficiency of the indirect power path, accounting for switching loss, ac magnetics loss, and other losses encountered by the indirect power transmitted at the switching

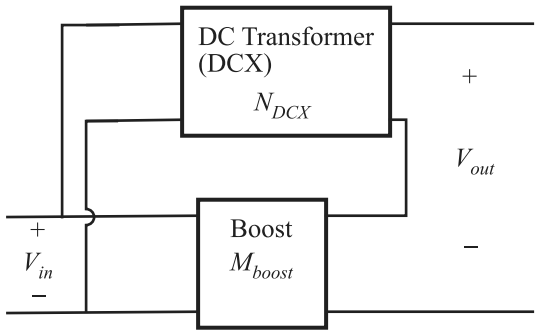

Fig. 2. Composite converter system design.

frequency. The averaged switch model of Fig. 1(b) neglects these losses and assumes that $\eta_{ac} = 1$. Dc losses such as semiconductor conduction losses and inductor dc resistance losses are also neglected in this figure.

The aforementioned discussion suggests that, to improve the efficiency of a boost converter operating with a high conversion ratio, the indirect power should be the minimum required to achieve the desired voltage gain at the given output power. Additionally, the path of the indirect power flow should be optimized to minimize ac losses (maximization of η_{ac}) as well as minimization of component stresses. These guiding principles provide the insight needed to develop an improved composite converter architecture using nonuniform modules. Modular system architectures that do not directly address the path of indirect power flow required by the application, and then tailor the modular architecture accordingly, can be expected to exhibit reduced efficiency and increased component stress.

With the concept of composite converter design, it is possible to limit the conversion ratio of each module to a smaller range, and therefore improve the system efficiency. One approach is shown in Fig. 2. A dc transformer (DCX) module is optimized to produce an isolated dc output voltage with a fixed voltage ratio N_{DCX} at very high efficiency [12]. This module generates the majority of the voltage gain of the boost system, and it performs most of the indirect power conversion of the system with an efficiency greater than that of a conventional boost converter. One possible realization of the DCX is the circuit illustrated in Fig. 3. With bidirectional power flow, this circuit is known as the dual active bridge [13], and can be designed for control of its output voltage. If the secondary-side switches are passive diodes or synchronous rectifiers without active control, then this circuit is a simple DCX; the converter can then be optimized to achieve very high efficiency and soft switching at points neighboring the current where the transformer currents are trapezoidal [14]–[16]. If we denote the boost module conversion ratio as M_{boost}, the system conversion ratio is $M = N_{\text{DCX}} + M_{\text{boost}}$. Therefore, to achieve same system conversion ratio, the boost module conversion ratio is much reduced, and the system efficiency can be improved.

However, since $M_{\text{boost}} \geq 1$, then when a system conversion ratio M less than $N_{\text{DCX}} + 1$ is required, the DCX module must be shut down, and the boost module alone produces the desired output voltage. Because the DCX output voltage is not

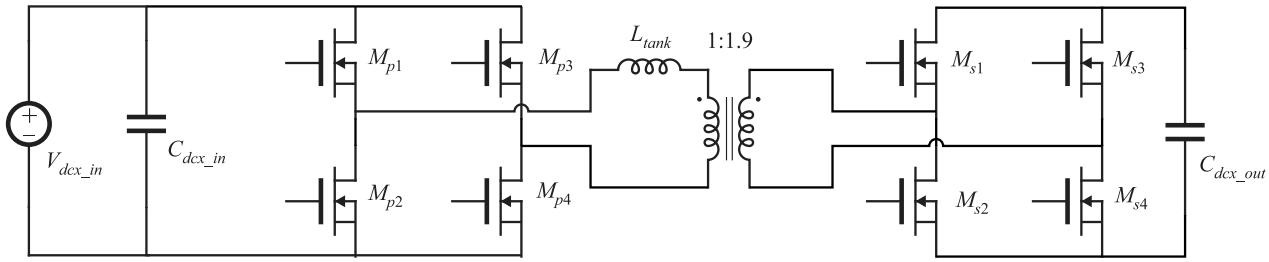

Fig. 3. Power stage of the dc transformer (DCX) module.

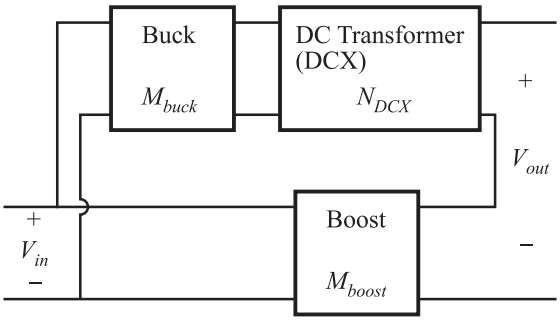

Fig. 4. Proposed composite converter system level architecture.

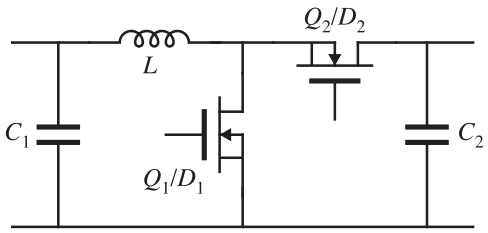

Fig. 5. Circuit diagram of power stage of the boost and buck modules.

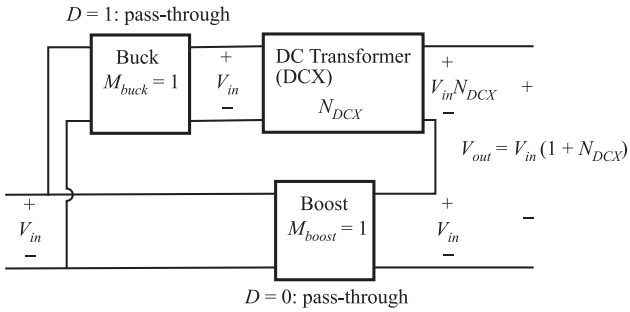

Fig. 6. Composite converter operation with both buck and boost module at pass-through.

controlled, this transition can be abrupt, and could lead to control difficulties. One way to mitigate this problem is to control the DCX output voltage. Another buck converter module is added before the DCX module, leading to the proposed composite converter architecture shown in Fig. 4. The buck converter module can adjust the DCX input voltage to enable smooth transitions between the modes. In particular, before turning DCX on or off, the DCX input voltage can be reduced to zero by the buck module. With smooth mode transitions, the composite converter is able to realize all conversion and control functions of a conventional boost converter.

In this discussion, we consider applications having bidirectional power flow, and hence the buck and boost modules share the same circuit topology illustrated in Fig. 5. An additional important benefit of adding the buck module is that the output voltage stress can be evenly shared between DCX and boost modules through variation of the buck conversion ratio, and therefore the transistor voltage stresses can be controlled to be half of the maximum output voltage. With the buck module, the DCX voltage stress can be controlled under all operating conditions, including light loads where DCX enters discontinuous-conduction-mode and its voltage conversion ratio increases. If we denote the conversion ratios of the buck and boost modules as M_{buck} and M_{boost}, respectively, then the system conversion ratio is $M = M_{\mathrm{buck}} N_{\mathrm{DCX}} + M_{\mathrm{boost}}$.

It is not necessary to switch all three modules at the same time. The buck and boost modules have highest efficiency in the pass-through mode ($M_{\mathrm{buck}} = 1$ or $M_{\mathrm{boost}} = 1$), where ac losses are zero and only conduction loss remains. This specific operating mode is illustrated as in Fig. 6; only the DCX operates (with optimized soft switching) and hence system efficiency is very high at this point. With pulse-width modulation of a buck or boost module at a duty cycle D near the pass-through value, the adjacent operating regions are expected to achieve high efficiency as well. For example, it is possible to operate the boost module in the pass-through mode when $M < 1 + N_{\mathrm{DCX}}$, and the buck module in the pass-through mode when $M > 1 + N_{\mathrm{DCX}}$. Furthermore, if the output voltage is lower than the boost module voltage rating, it is also possible to shut down both the buck and the DCX modules, and operate the boost module alone. Finally, if the input voltage is large, even when $M > 1 + N_{\mathrm{DCX}}$, it may still be necessary to operate buck module to limit the DCX output voltage within its voltage rating.

With this composite converter approach, both the power rating and the voltage rating of each module is reduced. Therefore, lower voltage devices, with reduced on-resistance as well as faster switching speed, can be used. Reactors can also be optimized with reduced power ratings and reduced applied voltages. It is also possible to design and optimize each module independently, according to their respective operating ranges. Although the system requires a larger number of power elements such as transistors, capacitors, etc., the sizes of these elements are reduced. The total power silicon area can be comparable to that of the conventional boost converter, but higher average efficiency is achieved.

With this architecture the number of capacitors is increased compared to the conventional boost converter. However, the voltage ratings and rms current ratings of the capacitors are substantially reduced, leading to a net reduction in capacitor size and cost. With the use of lower voltage semiconductors, the switching frequency of each module can be increased, which will reduce the required capacitance and inductance as well.

Several earlier approaches proposed in the literature can also achieve reduced device voltage ratings, through sharing of voltage stresses. For example, the multilevel converter [5], [17] can also reduce the device voltages, and hence utilize lower voltage devices. However, since the switch and capacitor rms current ratings are not reduced, the multilevel approach does not achieve the improvements in capacitor size and cost or in overall system efficiency that is possible using the proposed composite architecture. The modular converter system with input-parallel output-series configuration [18]–[20] is another popular approach to reduce device voltage stresses. However, since this approach does not address the indirect power flow and system ac power loss constraints, it is unable to achieve the high efficiencies over wide operating ranges as demonstrated here for the composite architecture.

III. Design Optimization

In many applications, although the system is designed to be able to handle worst case operating conditions such as maximum output power, maximum output voltage, etc., the system rarely operates at these points. For example, in solar power applications the peak insolation level may occur only for a short period, and most of the time the dc–dc converter operates at partial power. For traction motor drive applications, full power acceleration does not happen very frequently. Depending on the vehicle driving profile, the most frequent operating condition is at some intermediate power and voltage level. Therefore, it is desired to choose the composite converter system architecture so that it not only can handle the worst-case operating points, but also so that average loss is minimized under typical operating conditions. The composite boost architectures of Section II provide additional degrees of freedom that can be optimized to meet these goals.

We consider here an example in which the converter is required to process up to 10-kW output power. The input voltage is allowed to vary between 150 and 300 V. The boost ratio is between 1 and 3.8, while the maximum output voltage is limited to 800 V. However, most of the time, the converter is operated at neither maximum power nor maximum voltage.

It is desired to reduce the DCX and boost module voltage rating to 400 V, so that 600-V semiconductor devices can be utilized, according to the derating rule of our specified application. Therefore, at $V_{\rm out} = 800\,{\rm V}$, the output voltages of both the DCX and boost modules must be exactly 400 V, regardless of input voltage.

Since the system conversion ratio $M \leq 3.8$, at $V_{\rm out} = 800\,{\rm V}$, $V_{\rm in} \geq 211\,{\rm V}$. The DCX output voltage is limited to $V_{\rm DCX,out} = V_{\rm in} M_{\rm buck} N_{\rm DCX} = 400\,{\rm V}$. Since $M_{\rm buck} \leq 1$, this implies that $N_{\rm DCX} \geq 400/211 = 1.9$.

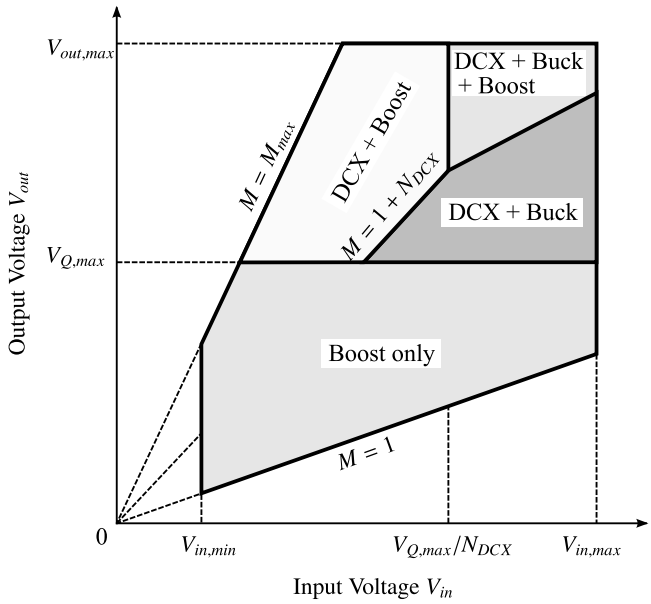

Fig. 7. Composite converter operating modes.

TABLE I
Module Specification Summary

DCX	Max. Input Voltage [V]	211
	Max. Output Voltage [V]	400
	Max. Output Current [A]	25
	Max. Input Current [A]	47.5
Boost	Max. Input Voltage [V]	300
	Max. Output Voltage [V]	400
	Max. Conversion Ratio	2.7
	Max. Input Current [A]	67
Buck	Max. Input Voltage [V]	300
	Max. Output Voltage [V]	211
	Min. Conversion Ratio	0.18
	Max. Output Current [A]	47.5

It is desired to maximize the boost plus DCX operating area to achieve lower DCX primary side transformer current and lower inductor current. Since the lowest conversion ratio the boost plus DCX mode can achieve is $M = N_{\rm DCX} + 1$, maximizing boost plus DCX operating area requires minimization of $N_{\rm DCX}$. At the same time, minimizing $N_{\rm DCX}$ also minimizes the operating area where the buck and boost modules operate simultaneously. Hence, switching loss is reduced as well.

Therefore, the minimum value $N_{\rm DCX} = 1.9$ is chosen. The operating modes of each converter module over the entire operating range are summarized in Fig. 7. When the output voltage is lower than 400 V, the boost module can operate alone, with DCX and buck modules shut down. When the output voltage is higher than 400 V, either the buck or the boost module is in the pass-through mode, depending on whether the system conversion ratio M is greater or less than $1 + N_{\rm DCX}$. If the input voltage is higher than 211 V, the buck converter will limit the DCX output to 400 V, and all three modules operate simultaneously.

For $N_{\rm DCX} = 1.9$, the rated operating conditions of each module are listed in Table I. With the module output voltage stress limited to 400 V, derated 600 V devices can be utilized. In the

TABLE II
COMPOSITE CONVERTER DESIGN SUMMARY

Buck / Boost	Number of MOSFETs	4
	Estimated total silicon area	265 mm^2
	Switching frequency	15 kHz
	Inductance	120 μH
	Inductor peak current	80 A
	Inductor winding	#44 Litz wire, 1000 strands
	Inductor core material	metal powder
	Inductor core volume	51 cm^3
DCX	Number of MOSFETs	12
	Estimated total silicon area	794 mm^2
	Switching frequency	33 kHz
	Transformer turns ratio	22:42
	Transformer winding	#44 Litz wire, 1500 strands on primary, 880 strands on secondary
	Transformer core material	ferrite
	Transformer core volume	72 cm^3

experimental prototype, 650-V 43-A superjunction MOSFETs are used. To meet the worst-case current rating, the buck and boost modules use two MOSFETs in parallel for each switch. The DCX module uses two MOSFETs in parallel for each switch at the primary side, and one MOSFET for each switch at the secondary side.

The detailed design of each module can now be optimized numerically, according to specified operating condition distribution. The loss model of each converter module has been well studied in the literature. For semiconductor loss, the conduction loss model is extracted from the device data sheet. The empirical switching loss model is curve fitted according to simulation models provided by the manufacturer. The core loss model is curve fitted according to material data sheet, while the reactor copper loss is calculated using Dowell's equation [21].

Partial power efficiency can be further optimized by use of the inductor current ripple to achieve zero-voltage switching at moderate-to-low currents. The body diodes of the superjunction MOSFETs exhibit significant reverse-recovery losses [22]. To optimize partial-power efficiency, the boost and the buck modules can be designed with negative instantaneous transistor current at the turn-on transitions to achieve zero-voltage switching at low to moderate power.

Due to the soft-switching behavior, the DCX module exhibits low switching loss. Therefore, the DCX module is able to operate at higher switching frequency, and ferrite core materials are employed for the DCX transformer and tank inductor. The tank inductor value is chosen to achieve zero-voltage switching of the MOSFET body diodes [14] and to minimize the transformer rms current at an intermediate power such that the system efficiency is optimized.

The resulting composite converter design parameters are summarized for this 10-kW prototype in Table II.

IV. COMPARISON WITH CONVENTIONAL BOOST CONVERTER

A. Switch Rms Current Comparison

To illustrate the benefits of reduction of indirect power achieved by the proposed composite converter architecture, the ideal switch rms currents in the composite converter are compared with those of a conventional boost converter, at a typical partial-power operating point, where $V_{\rm in} = 210\,{\rm V}$, $V_{\rm out} = 650\,{\rm V}$, at a 5-kW load. The comparison is summarized in Table III. The inductor current ripple is ignored in this comparison. Therefore, the data listed in the table is independent of the choice of devices, switching frequency, and magnetics design.

TABLE III
SWITCH RMS CURRENT COMPARISON AT 210-V INPUT, 650-V OUTPUT WITH 5-KW OUTPUT POWER

	System input current	23.8 A
	System output current	7.7 A
Conventional	Low-side switch	19.6 Arms
	High-side switch	13.5 Arms
Composite	Boost low-side switch	3.7 Arms
	Boost high-side switch	8.4 Arms
	Buck low-side switch	0 A
	Buck high-side switch	14.6 A (dc)
	DCX primary switch	14.6 Arms
	DCX secondary switch	7.7 Arms

The switch rms current in the boost module of the composite design is much reduced, relative to the conventional boost converter, while the buck module in pass-through mode only carries dc current. The DCX module can handle the trapezoidal current with ZVS at very high efficiency. Therefore, the proposed composite design has the potential to greatly reduce system ac power loss, and improve system efficiency. An additional benefit of the composite architecture is the ability to employ devices having lower voltage ratings and hence faster switching speed and lower switching loss.

B. Theoretical Efficiency Comparison

To compare the performance of the composite converter with a conventional approach, a similar 10-kW boost converter is designed using 1200-V IGBTs. The IGBT total silicon area is chosen to be the same as that of the composite converter design. The inductor core size is also chosen to have the same volume as the total reactor core volume in the composite converter design. Owing to the high switching loss of the IGBT, the switching frequency is limited to 10 kHz. The calculated efficiency is plotted versus input and output voltage at 5 kW, as shown in Fig. 8(a). It can be seen that the converter efficiency significantly drops as conversion ratio increases. For a fixed input / output voltage combination, the converter efficiency improves as output power increases, and it reaches peak efficiency at full power. At a typical partial-power operating point where $V_{\rm in} = 210\,{\rm V}$, $V_{\rm out} = 650\,{\rm V}$, at a 5 kW load, the efficiency is slightly less than 96%.

The calculated efficiency of proposed composite converter is plotted in Fig. 8(b), at 5 kW. The efficiency is generally higher than that of conventional boost converter, and the efficiency does not degrade significantly as conversion ratio increases. For fixed input / output voltage combination, the system peak efficiency occurs at some intermediate power level rather than at full power.

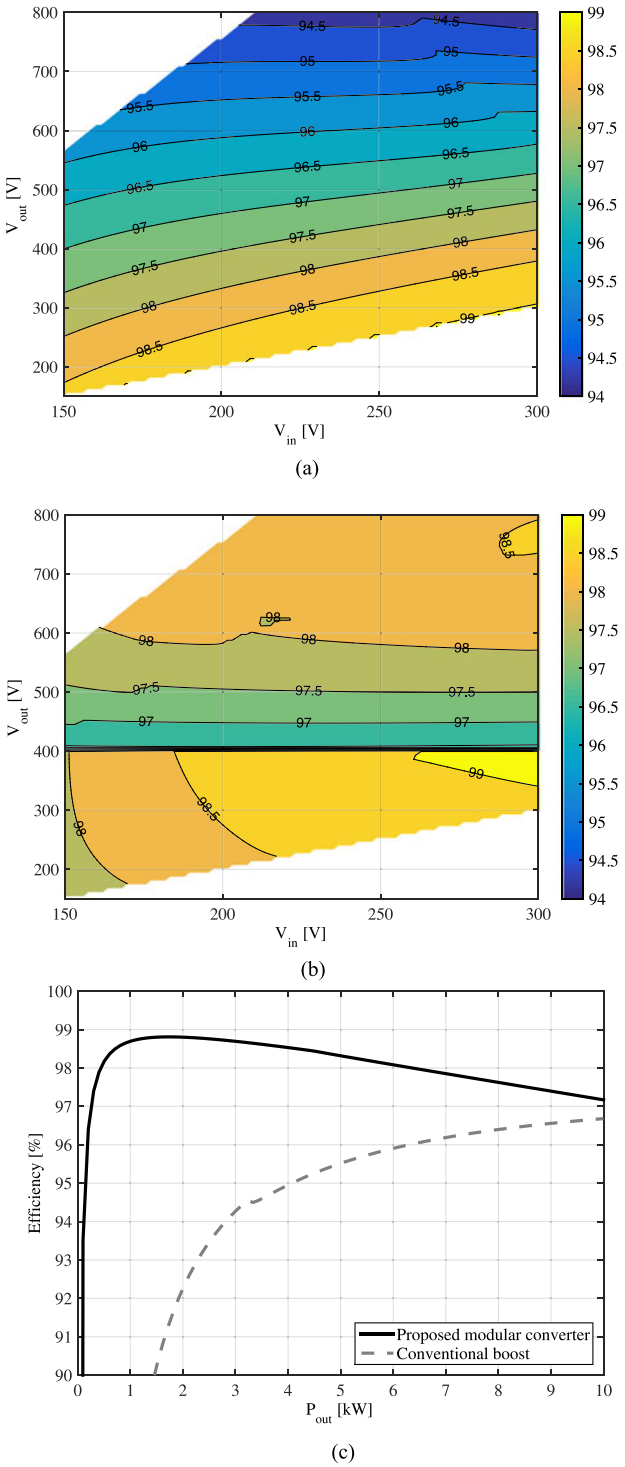

Fig. 8. Calculated converter efficiency. (a) Calculated conventional boost converter efficiency versus $V_{\rm in}$ and $V_{\rm out}$, at $P_{\rm out} = 5\,{\rm kW}$. (b) Calculated composite converter efficiency versus $V_{\rm in}$ and $V_{\rm out}$, at $P_{\rm out} = 5\,{\rm kW}$. (c) Efficiency versus $P_{\rm out}$, at $V_{\rm in} = 210\,{\rm V}$ and $V_{\rm out} = 650\,{\rm V}$ for both converters.

At operating point where $V_{\rm in} = 210\,{\rm V}$, $V_{\rm out} = 650\,{\rm V}$, at a 5 kW load, the efficiency is approximately 98.5%.

Fig. 8(c) compares the efficiency of the conventional boost converter and the proposed composite converter versus output power, with fixed $V_{\rm in} = 210\,{\rm V}$ and $V_{\rm out} = 650\,{\rm V}$. Although for

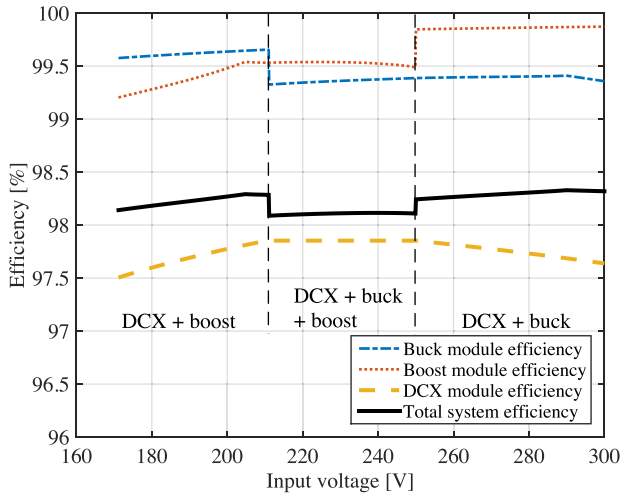

Fig. 9. Calculated converter module efficiency and total system efficiency as functions of the input voltage, at $V_{\rm out} = 650\,{\rm V}$, $P_{\rm out} = 5\,{\rm kW}$.

the composite converter the full power efficiency is only 0.5% higher than conventional boost converter, the efficiency at partial power is much higher. In an application in which the power varies substantially, the superior partial-power characteristic of the composite converter approach can lead to major reductions in the average loss.

Fig. 9 shows efficiency of each converter module in different operation modes as functions of the input voltage, at fixed 650-V output voltage, 5-kW output power. Since the buck and the boost module process only partial power with conversion ratios close to one, their efficiencies are very high.

C. Capacitor Rating Comparison

With reduced module voltage stress, the capacitor voltage ratings in the composite converter can also be reduced. In comparison to the conventional boost converter, the modules of the composite converter employ higher switching frequencies and therefore the capacitances can be reduced as well, while maintaining the same output voltage ripple. Therefore, although the composite converter employs an increased number of individual capacitor elements, the total capacitor energy storage rating can be lower than conventional boost converter.

In a typical boost converter, the output capacitor rms current rating typically constrains the capacitor size and cost, rather than the capacitance itself. Since rms capacitor current is independent of the switching frequency, simply increasing the switching frequency will not reduce the capacitor size. In pass-through mode, the buck or boost modules do not apply ac currents to their capacitors, and operating points near pass-through mode exhibit low rms capacitor currents. The DCX module exhibits relatively low capacitor rms currents as well, particularly when the transformer winding currents are trapezoidal. Hence, the capacitor rms current requirements are substantially lower than in the conventional boost converter operating at high duty cycle.

The minimum capacitance required to achieve a worst case $\pm 5\,{\rm V}$ output voltage ripple is calculated, for both the

TABLE IV
CAPACITOR RATING FOR CONVENTIONAL AND COMPOSITE CONVERTERS

		Voltage rating [V]	RMS current rating [A]	Minimum capacitance required [μF]
Conventional	Input	300	6	100
	Output	800	57.3	300
Composite	Input	300	40	100
	Buck output	210	21	300
	DCX output	400	5	100
	Boost output	400	34	222

TABLE V
TOTAL CAPACITOR ENERGY AND POWER RATING COMPARISON

	Total capacitor energy storage rating [J]	Total capacitor power rating [kW]
Conventional	100.5	47.7
Composite	36.2	37.1

conventional boost converter and the proposed composite converter. The rms current rating for each capacitor is calculated as well, and the results are listed in Table IV, for the specific 10 kW application. It is assumed that a fixed 100 μF input capacitor is used for both cases.

The energy storage rating is calculated as $0.5\,CV_{\mathrm{rate}}^2$, while the power rating is calculated as $V_{\mathrm{rated}}I_{\mathrm{rms,rated}}$. The total capacitor energy storage ratings and power ratings are summarized in Table V. The composite converter requires both lower energy and power ratings, which can lead to reduced capacitor cost.

V. EXPERIMENTAL RESULTS

The 10 kW composite converter example described earlier has been built. Its open-loop operation has been demonstrated and tested in all operating modes.

Fig. 10 shows the operation in DCX plus boost mode. The DCX waveforms are shown in the upper half of the figure, operating at 210-V input and 400-V output. Both the primary and secondary side devices of the DCX operate with ZVS, as implied by the smooth transition of switching node voltages. The secondary side switching node voltage is measured with a differential probe, with reference to the negative output of the DCX. The buck and boost module waveforms are shown in the lower half of the figure. The buck module operates in pass-through mode, with high-side MOSFET constantly on, and only dc current flowing through inductor. The boost module operates with 210-V input and 250-V output, and therefore the total output voltage is 650 V. At this operating point, the output power is approximately 5 kW, and the boost module operates in boundary conduction mode.

Fig. 11 shows operation in DCX plus buck mode. The system input voltage is approximately 210 V. The buck module operates with approximately 50% duty cycle, while the boost module operates in pass-through mode. The DCX operates at

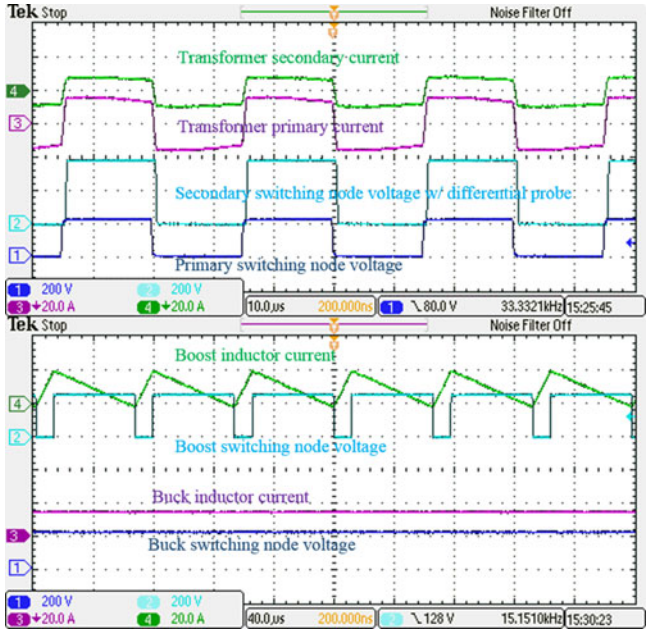

Fig. 10. Composite converter operation in DCX + boost mode.

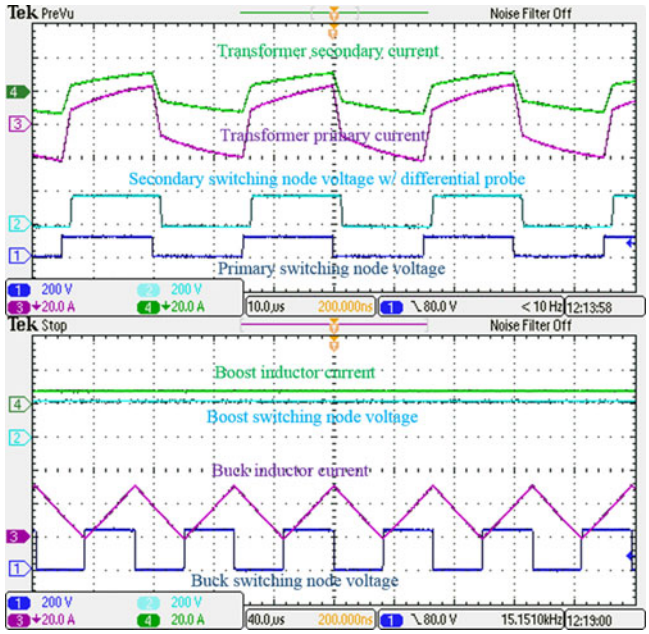

Fig. 11. Composite converter operation in DCX + buck mode.

approximately 100-V input and 190-V output. The total system output voltage is 410 V.

Fig. 12 illustrates operation in DCX plus buck plus boost mode. The system input voltage is 230 V. The buck module output is 210 V, while both the boost and DCX module outputs are 400 V. The total system output is 800 V.

Fig. 13 plots the measured efficiency with different input / output voltages, at fixed 5 kW output power. The highest efficiency recorded is 98.7%, at approximately 210-V input and 650-V output. All points with output voltage greater than 500 V achieve measured efficiency higher than 98%. When the output

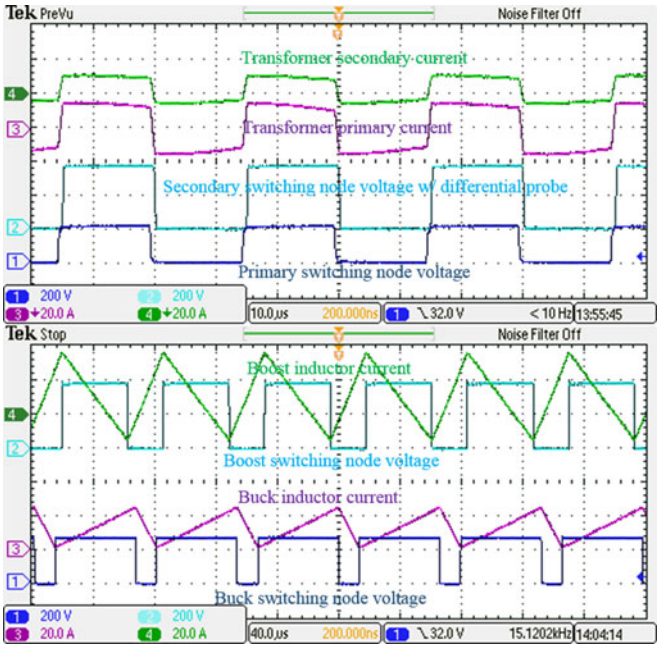

Fig. 12. Composite converter operation in DCX + buck + boost mode.

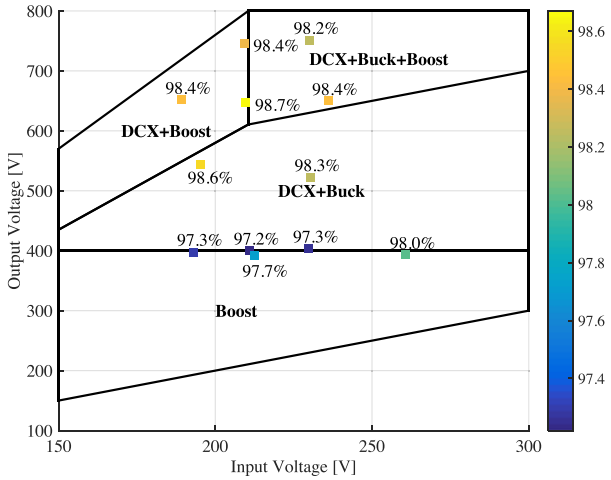

Fig. 13. Measured composite converter efficiency versus V_{min} and V_{out}, at $P_{\mathrm{out}} = 5$ kW.

voltage is slightly above 400 V, and the system operates in DCX plus buck mode, the efficiency slightly drops to 97.2%, due to the small buck module conversion ratio. However, when the output voltage is below 400 V, the system can operate in boost only mode, and the measured efficiency is higher.

Fig. 14 shows the measured efficiency versus output power at different input/output voltages and different operating modes. The measured results are compared with theoretical model used in design. The measurements show slightly higher efficiency than theoretical calculation. This is mainly because the actual semiconductor junction and copper winding temperatures in the experiment are lower compared to the worst-case values assumed in the theoretical model. As a result, the actual conduction losses are slightly lower compared to the model.

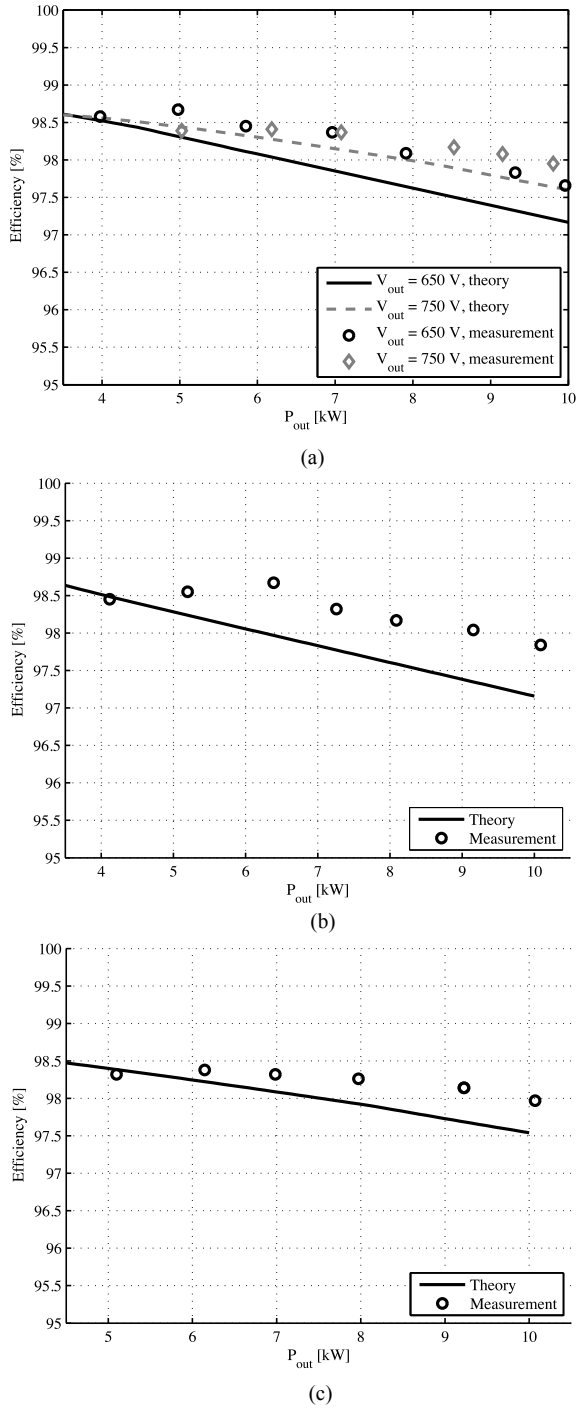

Fig. 14. Measured converter efficiency versus output power. (a) $V_{\mathrm{in}} = 210$ V. Converter operates at DCX + boost mode. (b) $V_{\mathrm{in}} = 260$ V, $V_{\mathrm{out}} = 650$ V. Converter operates at DCX + buck mode. (c) $V_{\mathrm{in}} = 260$ V, $V_{\mathrm{out}} = 750$ V. Converter operates at DCX + buck + boost mode.

VI. Conclusion

In this paper, a novel dc–dc boost composite converter architecture is proposed. It consists of one buck module, one boost module and one DCX module. With this architecture, each module operates with reduced power rating as well as reduced voltage rating. The efficiency of each module can be improved. This enables system level optimization and employment of module

pass-through modes to achieve high efficiency over a wide range of partial power operating conditions. The system efficiency can be optimized according to application-specific operating condition distributions. The proposed composite converter also has the potential to reduce total capacitor volume and cost.

To verify the claimed high efficiency, a 10-kW composite converter has been designed and constructed. Its theoretical performance is compared with conventional boost converter, with same total semiconductor silicon area as well as same total reactor core volume. Significant efficiency improvement is observed in simulation. The open-loop operation is verified in experiments, with different operating modes, and high efficiencies are recorded. With a 3:1 boost ratio, and 50% of rated power, 98.7% efficiency is achieved.

REFERENCES

[1] R. Bründlinger, N. Henze, H. Häberlin, B. Burger, A. Bergmann, and F. Baumgartner, "prEN 50530—The new European standard for performance characterisation of PV inverters," in *Proc. 24th Eur. Photovoltaic Solar Energy Conf.*, 2009, pp. 3105–3109.

[2] B. Brooks and C. Whitaker, "Guideline for the use of the performance test protocol for evaluating inverters used in grid-connected photovoltaic systems," California Energy Commission. (2005, Feb.). [Online]. Available: http://www.gosolarcalifornia.ca.gov/equipment/documents/Sandia_Guideline_2005.pdf

[3] K. Muta, M. Yamazaki, and J. Tokieda, "Development of new-generation hybrid system THS II—Drastic improvement of power performance and fuel economy," power performance and fuel economy," SAE Tech. Rep. no. 2004-01-0064, 2004.

[4] Y. Tsuruta, Y. Ito, and A. Kawamura, "Snubber-assisted zero-voltage and zero-current transition bilateral buck and boost chopper for EV drive application and test evaluation at 25 kW," *IEEE Trans. Ind. Electron.*, vol. 56, no. 1, pp. 4–11, Jan. 2009.

[5] J. Itoh, K. Matsuura, and K. Orikawa, "Reduction of a boost inductance using a switched capacitor DC-DC converter," in *Proc. Power Electron. ECCE Asia,* 2011, pp. 1315–1322.

[6] M. Hirakawa, M. Nagano, Y. Watanabe, K. Andoh, S. Nakatomi, and S. Hashino, "High power density DC/DC converter using the close-coupled inductors," in *Proc. Energy Convers. Congr. Expo.,* 2009, pp. 1760–1767.

[7] T. Kawashima, S. Funabiki, and M. Yamamoto, "Recovery-less boost converter for electric vehicle," in *Proc. Power Electron. Appl. Eur. Conf.,* 2009, pp. 1–10.

[8] Y. Tsuruta and A. Kawamura, "A novel soft switching scheme QRAS converter aimed for FCEV," in *Proc. Power Electron. Spec. Conf.,* 2005, pp. 779–785.

[9] F. Krismer, J. Biela, and J. Kolar, "A comparative evaluation of isolated bi-directional DC/DC converters with wide input and output voltage range," in *Proc. Ind. Appl. Conf.,* 2005, pp. 599–606.

[10] R. W. Erickson and D. Maksimovic, *Fundamentals of Power Electronics*. New York, NY, USA: Springer, 2001.

[11] D. Wollaver, "Fundamental study of dc to dc conversion system," Ph.D. dissertation, Dept. Elect. Eng., Massachusetts Inst. Technol., Cambridge, MA, USA, 1969.

[12] R. White, "Emerging on-board power architectures," in *Proc. IEEE Appl. Power Electron. Conf.*, 2003, pp. 799–804.

[13] R. De Doncker, D. Divan, and M. Kheraluwala, "A three-phase soft-switched high-power-density DC/DC converter for high-power applications," *IEEE Trans. Ind. Appl.*, vol. 27, no. 1, pp. 63–73, Jan./Feb. 1991.

[14] D. Jones and R. Erickson, "Analysis of switching circuits through incorporation of a generalized diode reverse recovery model into state plane analysis," *IEEE Trans. Circuits Syst. I*, vol. 60, no. 2, pp. 479–490, Feb. 2013.

[15] S. Inoue and H. Akagi, "A bi-directional isolated DC/DC converter as a core circuit of the next-generation medium-voltage power conversion system," in *Proc. Power Electron. Spec. Conf.,* 2006, pp. 1–7.

[16] D. Costinett, D. Maksimovic, and R. Zane, "Design and control for high efficiency in high step-down dual active bridge converters operating at high switching frequency," *IEEE Trans. Power Electron.*, vol. 28, no. 8, pp. 3931–3940, Aug. 2013.

[17] E. Deschamps and I. Barbi, "A flying-capacitor ZVS PWM 1.5 kW DC-to-DC converter with half of the input voltage across the switches," *IEEE Trans. Power Electron.*, vol. 15, no. 5, pp. 855–860, Sep. 2000.

[18] G. Ortiz, J. Biela, D. Bortis, and J. Kolar, "1 megawatt, 20 kHz, isolated, bidirectional 12 kV to 1.2 kV DC-DC converter for renewable energy applications," in *Proc. Int. Power Electron. Conf.*, Jun. 2010, pp. 3212–3219.

[19] J. Kimball, J. Mossoba, and P. Krein, "A stabilizing, high-performance controller for input series-output parallel converters," *IEEE Trans. Power Electron.*, vol. 23, no. 3, pp. 1416–1427, May 2008.

[20] A. Chub, O. Husev, and D. Vinnikov, "Input-parallel output-series connection of isolated quasi-Z-source DC-DC converters," in *Proc. Electr. Power Quality Supply Rel. Conf.,* Jun. 2014, pp. 277–284.

[21] P. Dowell, "Effects of eddy currents in transformer windings," *Proc. Inst., Electr. Eng.,* vol. 113, no. 8, pp. 1387–1394, Aug. 1966.

[22] R. Burra and K. Shenai, "CoolMOS integral diode: A simple analytical reverse recovery model," in *Proc. Power Electron. Spec. Conf.,* 2003, pp. 834–838.

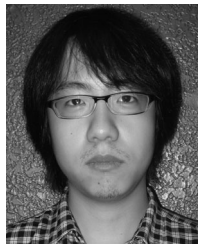

Hua Chen (S'09) received the B.Eng. degree from the Chinese University of Hong Kong, Hong Kong. From spring 2012, he is working toward the Ph.D. degree at the Department of Electrical, Computer and Energy Engineering, University of Colorado, Boulder, CO, USA.

His research interests include high efficiency dc–dc converter for electric vehicles and power management IC design.

Kamal Sabi received the B.S. and M.S. degrees in electrical engineering from the University of Colorado, Boulder, CO, USA.

He served as a Professional Research Assistant at the Colorado Power Electronics Center (2012–2014) where he worked on designing and implementing high efficient dc–dc converter systems for electric vehicles. He is currently working as a SCADA System Engineer at TECHNEAUX, Lafayette, LA, USA.

Hyeokjin Kim (S'15) received the B.Sc. and M.Sc. degrees in electrical engineering from Hongik University, Seoul, South Korea, in 2009 and 2011, respectively. He is currently working toward the Ph.D. degree at the University of Colorado, Boulder, CO, USA.

His research interests include converter design, digital control, modeling, energy harvesting.

Tadakazu Harada received the B.S. degree from the Tokyo University of Agriculture and Technology, Tokyo, Japan, and the M.S. degree from the University of Colorado, Boulder, CO, USA.

In 2006, he joined Toyota Motor Corporation. His research is on development of the power module for hybrid systems. During 2013–2014, he also worked on power electronics for automobile applications.

Robert Erickson (M'84–SM'99–F'00) received the B.S., M.S., and Ph.D. degrees from the California Institute of Technology, Pasadena, CA, USA.

Since 1982, he has been on the faculty of the ECEE Department, University of Colorado, Boulder, CO, USA, where he served as Chair in 2002–2006 and 2014–2015. He and Maksimovic codirect the Colorado Power Electronics Center. His research interests include electric vehicle power electronics (charger and drive train power conversion), grid interface of solar and wind power systems, low harmonic rectification, resonant power conversion, and power electronics modeling and control. He is an Author of the textbook *Fundamentals of Power Electronics* (New York, NY, USA: Springer, 2001).

Dr. Erickson is a Fellow of the UC-B/NREL Renewable and Sustainable Energy Institute.

Dragan Maksimovic (M89–SM04–F15) received the B.S. and M.S. degrees in electrical engineering from the University of Belgrade, Belgrade, Serbia, in 1984 and 1986, respectively, and the Ph.D. degree from the California Institute of Technology, Pasadena, CA, USA, in 1989.

From 1989 to 1992, he was with the University of Belgrade. Since 1992, he has been with the Department of Electrical, Computer and Energy Engineering, University of Colorado, Boulder, CO, USA, where he is currently a Professor and Codirector of the Colorado Power Electronics Center. His current research interests include power electronics for renewable energy sources and energy efficiency, high frequency power conversion using wide bandgap semiconductors, digital control of switched-mode power converters, as well as analog, digital and mixed-signal integrated circuits for power management applications. He has coauthored more than 250 publications and the textbook *Fundamentals of Power Electronics* (New York, NY, USA: Springer, 2001).

Dr. Maksimovic received the 1997 NSF CAREER Award, the IEEE PELS Transactions Prize Paper Award in 1997, the IEEE PELS Prize Letter Awards in 2009 and 2010, the University of Colorado Inventor of the Year Award in 2006, the IEEE PELS Modeling and Control Technical Achievement Award for 2012, the Holland Excellence in Teaching Awards in 2004 and 2011, the Charles Hutchinson Memorial Teaching Award for 2012, and the 2013 Boulder Faculty Assembly Excellence in Teaching Award.